REPORT DOCUMENTATION PAGE

Form Approved
OMB No. 0704-0188

1. REPORT DATE *(DD-MM-YYYY)*	2. REPORT TYPE	3. DATES COVERED *(From - To)*
11-02-2015	Final	12-01-11 to 11/30/14

4. TITLE AND SUBTITLE
Seabed Characterization for SW2013 Mid_Frequency Reverberation Experiment

5a. CONTRACT NUMBER

5b. GRANT NUMBER
N00014-12-1-0082

5c. PROGRAM ELEMENT NUMBER

6. AUTHOR(S)
Charles W. Holland

5d. PROJECT NUMBER
19521

5e. TASK NUMBER

5f. WORK UNIT NUMBER

7. PERFORMING ORGANIZATION NAME(S) AND ADDRESS(ES)
The Pennsylvania State University Applied Research Labotatory
Office of Sponsored Programs
110 Technology Center Building
University Park, PA 16802-7000

8. PERFORMING ORGANIZATION REPORT NUMBER

9. SPONSORING/MONITORING AGENCY NAME(S) AND ADDRESS(ES)
Office of Naval Research
875 North Randolph Street
Arlington, VA 22203-1995

10. SPONSOR/MONITOR'S ACRONYM(S)
ONR

11. SPONSORING/MONITORING AGENCY REPORT NUMBER

12. DISTRIBUTION AVAILABILITY STATEMENT
DIstribution Unlimited

13. SUPPLEMENTARY NOTES

14. ABSTRACT
Seabed geoacoustic structure exhibits variability on a wide spectrum of spatial scales. An experiment was designed and conducted (under the TREX13 experiment) to measure those scales in an inner shelf ridge and swale environment off the coast of Panama City, Florida. One of the surprising results was the observation that significant scales of lateral variability in the sub-bottom exist at scales of 1-10 m. This was observed at both measurement sites, one on a small ridge and one in a swale. Very large differences were observed between the gross sediment properties on the ridge and in the swale despite there being only 30 cm difference in water depth between them. Some of the physical properties could be estimated, but many of the geoacoustic results are rather qualitative. New techniques are required for fully quantifying the geoacoustic variability in such a heterogeneous environment.

15. SUBJECT TERMS

16. SECURITY CLASSIFICATION OF:			17. LIMITATION OF ABSTRACT	18. NUMBER OF PAGES	19a. NAME OF RESPONSIBLE PERSON
a. REPORT	b. ABSTRACT	c. THIS PAGE	SAR	8	Charles W. Holland
U	U	U			19b. TELEPONE NUMBER *(Include area code)* 814 865-1724

Seabed Characterization for SW2013 Mid-Frequency Reverberation Experiment

Charles W. Holland

The Pennsylvania State University
Applied Research Laboratory
P.O. Box 30, State College, PA 16804-0030
Phone: (814) 865-1724 Fax (814) 863-8783 email: holland-cw@psu.edu

Grant Number: N00014-12-1-0082

LONG TERM GOALS

The long-term science question addressed by the SW2013 experiment (relevant to this proposal) is to advance understanding of the seabed mechanisms that control clutter and diffuse reverberation

OBJECTIVES

The specific goals are to: 1) quantify seabed physical properties and their spatial (vertical and horizontal) variability and uncertainties and 2) based on the spatial variability make and test hypotheses about the mechanisms that control clutter and diffuse reverberation.

APPROACH

The observational approach is based on direct path measurements of seabed reflection. The key advantages of this approach are: high resolution (0.1 m vertically, 1-10 m laterally); relatively modest uncertainties [1] including those from the space/time varying oceanography and biology; and that low source levels are possible. The main challenge is that water depth, 20 m, is 4 times smaller than what has been achieved in the past which poses challenges for multipath separation and separation of angle dependence from lateral variability. The latter problem arises due to the small Fresnel zone size coupled with the shorter scales of seabed lateral variability that occur for inner shelf environments.

WORK COMPLETED

The tasks in FY14 were analysis of TREX13: 1) wide angle seabed reflection data and 2) normal incidence seabed reflection data.

RESULTS

Wide angle seabed reflection measurements
Wide angle seabed reflection data collected and processed in FY13 were analyzed to extract the geoacoustic properties as a function of depth and frequency at two sites: one on a ridge crest along the clutter track, and one in a swale near the main reverberation line, see Fig 1.

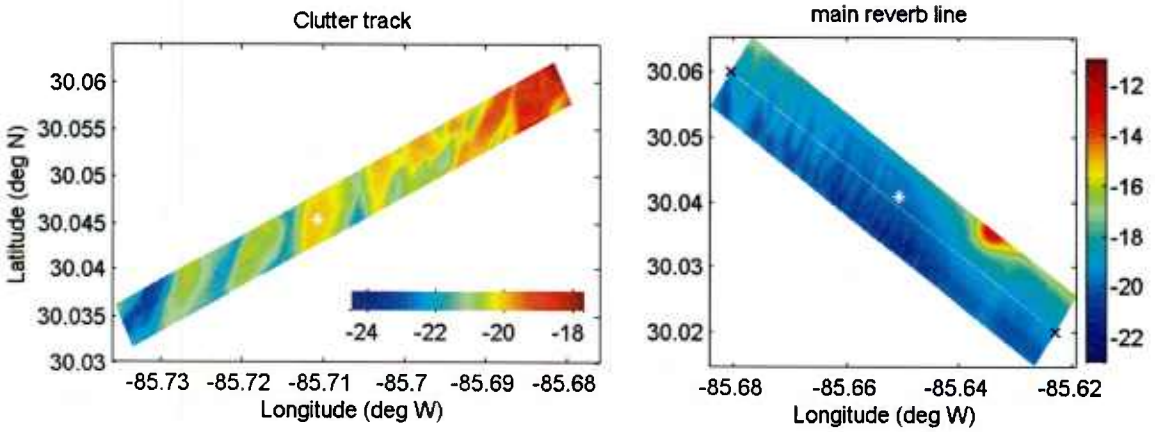

Figure 1. TREX bathymetry (from DeMoustier and Kraft) with wide angle reflection sites (*) along clutter track (Site C) and main reverberation line (Site 2).

Measured reflection coefficient data **R** as a function of frequency (1.4 – 12 kHz) and angle (15-47°) at Site 2 are shown in Fig 2a. Before discussing these data, it is helpful to consider measurements from a mid-shelf region (Fig 2b), which show an interference pattern caused by classical quarter-wave ($k_{jz}d_j=m\pi/2$) and half-wavelength resonances ($k_{jz}d_j=m\pi$) where k_{jz} is the vertical component of the wavenumber in the jth layer, d_j is layer thickness, and m is an integer. From these simple equations, it can be seen that the evolution of these resonances across frequency/angle space is a function of the layer sound speed and thickness. The amplitudes of the peaks and valleys can be shown to be a function of the attenuation and the density. Thus, wide angle reflection data contain a great deal of information about the geoacoustic properties; for example, with known angle and frequency, the data immediately yield sound speed and layer thickness. Over the years, a robust probabilistic approach has been developed to capture all the geoacoustic properties and their uncertainties (e.g., see [2]). However, this approach failed on the data shown in Fig 2a. This was surprising inasmuch as dozens of prior measurements (of which Fig 2b is one example) have always yielded meaningful results. These measurements have been conducted in a wide variety of settings in widely varying locations (Straits of Sicily, the northern Tyrrhenian Sea, the New Jersey shelf, and the Scotian Shelf). One significant difference is that our prior measurements were all on the mid to outer shelf (80-180 m water depth).

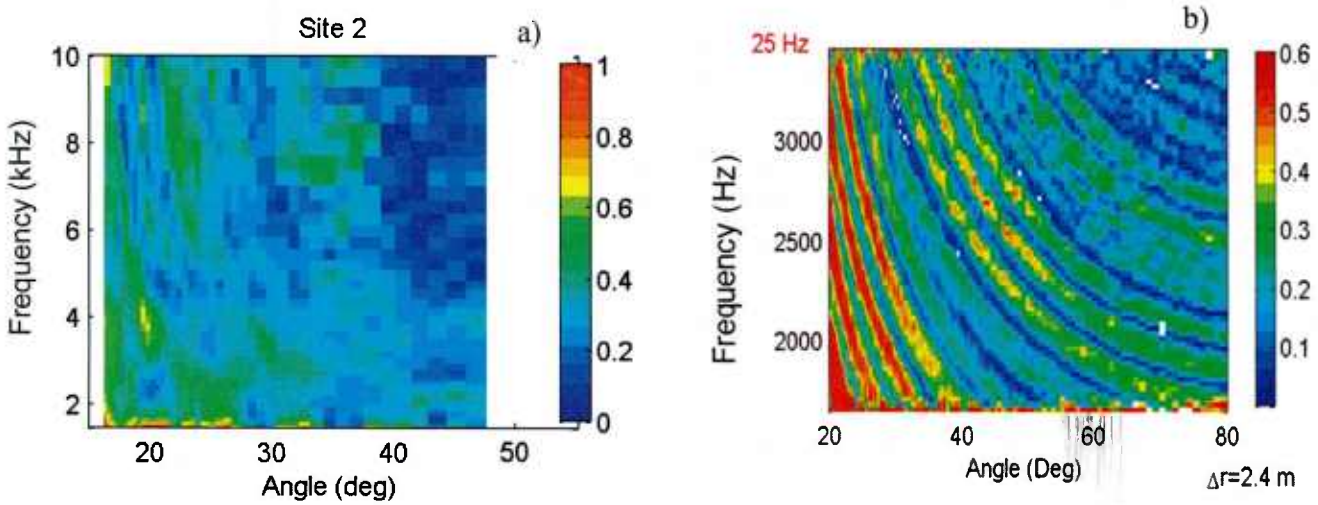

Figure 2 seabed reflection coefficient at a) TREX13 Site 2 and b) on the mid-shelf south of Sicily.

The reason why our method failed was that (for the first time in our experience), the assumption of a plane-layered medium failed (which is assumed in our forward model). For example note that in Fig 2a, below about 38° there is evidence of resonance effects due to layering. However, at and above 38°, the evolution of the resonances changes. This non-stationarity in **R** means that the across the relatively small aperture of the measurement (spanning just 18 m) there is a marked change in the layering structure of the seabed. Variable bathymetry was investigated as being an alternative contributor to the spatially non-stationary data; however the de Moustier/Kraft multibeam data showed a flat bottom with a small slope, 0.1°. An additional piece of evidence that supports variable sub-bottom structure is that the seabed reflected path arrival times are consistent with a flat and only slightly tilted seabed.

Though the planned geoacoustic analysis is not possible, the data reveal a valuable and important seabed characteristic, namely that there is significant lateral variability in the swale on lateral scales of 1-10 m. This scale of variability is expected to impact both propagation and reverberation.

The measured data do provide a rough indication or limit on the sound speed. Due to the absence of a critical angle at Site 2 above ~16°, the sound speed must be less than about 1585 m/s. Wide angle reflection measurements at the crest of the clutter site showed a markedly different critical angle, corresponding to a sound speed roughly of 1680 m/s. However, the full geoacoustic inversion technique at the clutter site also failed; its frequency-angle behavior also showed strong lateral seabed variability at the 1-10 m scale which explains the failure of the method.

Normal incidence seabed reflection coefficients

Normal incidence reflectivity was measured as shown in Figure 3 where the source and receiver were suspended below a small catamaran (about 2 x 2 m) which was towed behind R/V Quest at about 3 knots. The source was the same used for the wide angle measurements but the receiver was a hydrophone approximately 2 m above the source on the same tow line. The system was towed along 7 bearings at 3 sites, but equipment problems rendered data only along one leg at one site viable. Fortuitously, this leg (black line in Figure 4a) was close to the Site 2 wide angle reflection track (short red line). Thus, part of the analysis motivation was to detect laterally varying seabed structure that could be responsible for the non-stationarity of the reflection data (e.g., Figure 2a at 38°).

The magnitude of the peak broadband (1.4-12 kHz) bottom reflection coefficient was formed by taking the ratio on every ping of the bottom reflected path and the direct path (see Fig 3), correcting each for spherical spreading. Source amplitude variations were negligible, but were accounted for. The results were initially averaged over a lateral extent on the seabed of ~2.25 m (3 pings) and are shown in Figure 4b (blue line). Note the substantial drop in reflectivity at ~13.36 hr., where the change is almost a factor of 2 in amplitude. Both system (e.g., source depth or amplitude variation) and environmental factors to explain this drop were explored. It was concluded that the observed variations are not due system effects; both the source and receiver were essentially omnidirectional, so motion from towing would have negligible impact and the source-receiver positions were carefully measured on each ping. The variability in the reflection coefficient must be due to seabed effects.

The two strong reflection peaks at ~ hour 13.385 were examined on an individual ping basis and it was found that these peaks occur at single pings (Fresnel zone about 1.5 m). This 'glint-like' behavior together with the non-negligible overlap in seabed illuminated area between pings can most easily be explained by focusing from bathymetric curvature. The increased reflectivity at hour 13.39 by contrast occurs over many consecutive pings and has a spectral peak around 4-5 kHz, whereas the rest of the

track has its main spectral content at 2-4 kHz. The specific cause of the 4-5 kHz peak is not known at present, but seems likely due to sediment geoacoustic variability, possibly due to changes in layering.

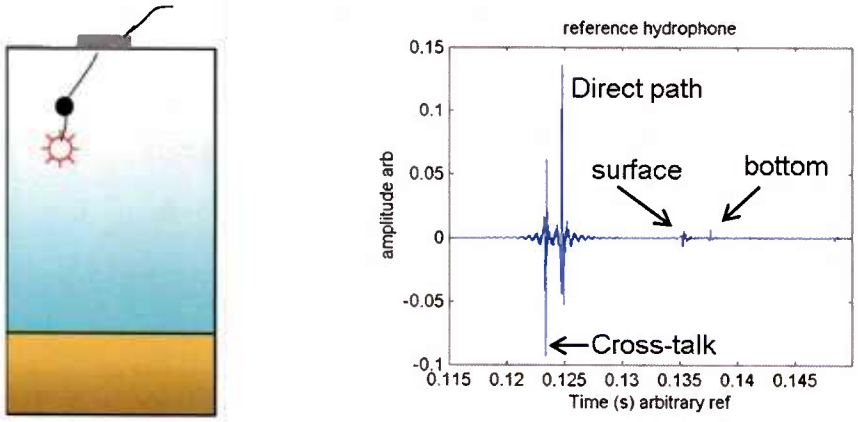

Figure 3 a) cartoon of normal incident seabed reflection experiment. The source (red) is nominally at a depth of 10.2 m and the receiver (●) is 2.17m above the source. The source depth varied by ±0.5 m but is known to high precision being measured both by a pressure sensor and acoustically using time of flight to known boundaries (sea surface and bottom). The relative source-receiver distance had very small oscillatory excursions during the run of ±0.015 m. b) A typical example of the received signal showing the direct, surface, and bottom reflected paths.

There is a spatial periodicity clearly observed in the reflection data (see blue curve in Fig. 4b). The main peak of the spatial periodicity is at 26 m with a secondary peak at 43 m [3]. These periodicities do not correspond with any motion of the source or receiver, thus they are not artifacts related to system effects. It is possible that there are small scale bedforms unresolved in the bathymetry leading to either slight focusing and defocusing or that the bedforms or other processes lead to fluctuations on that scale.

A comparison between reflectivity and bathymetry is shown in Fig 4c. It should be noted first that the reflection data positions may be biased forward along the track by a few meters (perhaps up to 10 m). That is, the source and receiver trailed slightly (an unknown distance) behind the GPS sensor fixed on the back of the catamaran. Positional errors on the extracted multibeam data are unknown but presumably small. It is important to observe that the bathymetry varies only 30 cm along the track; the changes are minor.

One salient point is the lack of obvious correlation between the reflection coefficient and the bathymetry. The sand ridge crest peak (13.342 hr.) is separated by more than 80 m from the peak of the reflection coefficient (13.358 hr.). Also, near the end of the track, there is a sharp rise in the reflection coefficient, but the bathymetry is nearly flat. Only the central and lowest part of the track has a reasonable correlation with the lowest reflection coefficient values.

The reflection data suggest four regimes, which are delineated in Fig 4b,c in the vertical dotted cyan lines and numbered 1 to 4. Regime 1 seems related to the sand ridge crest, but oddly, the reflection coefficient steadily increases from the stoss side to almost precisely halfway down the lee side (from ridge peak to trough). At this point there is a rapid drop in reflectivity and this zone is called Regime 2.

Regime 3 has generally low reflectivity values (with many peaks) and corresponds with the deepest part of the bathymetry. At about 13.402 hr, the reflectivity rises sharply (Regime 4) even faster than the decline in Regime 2. The final portion of the track looks similar in reflectivity values to Regime 1, though with a steeper slope.

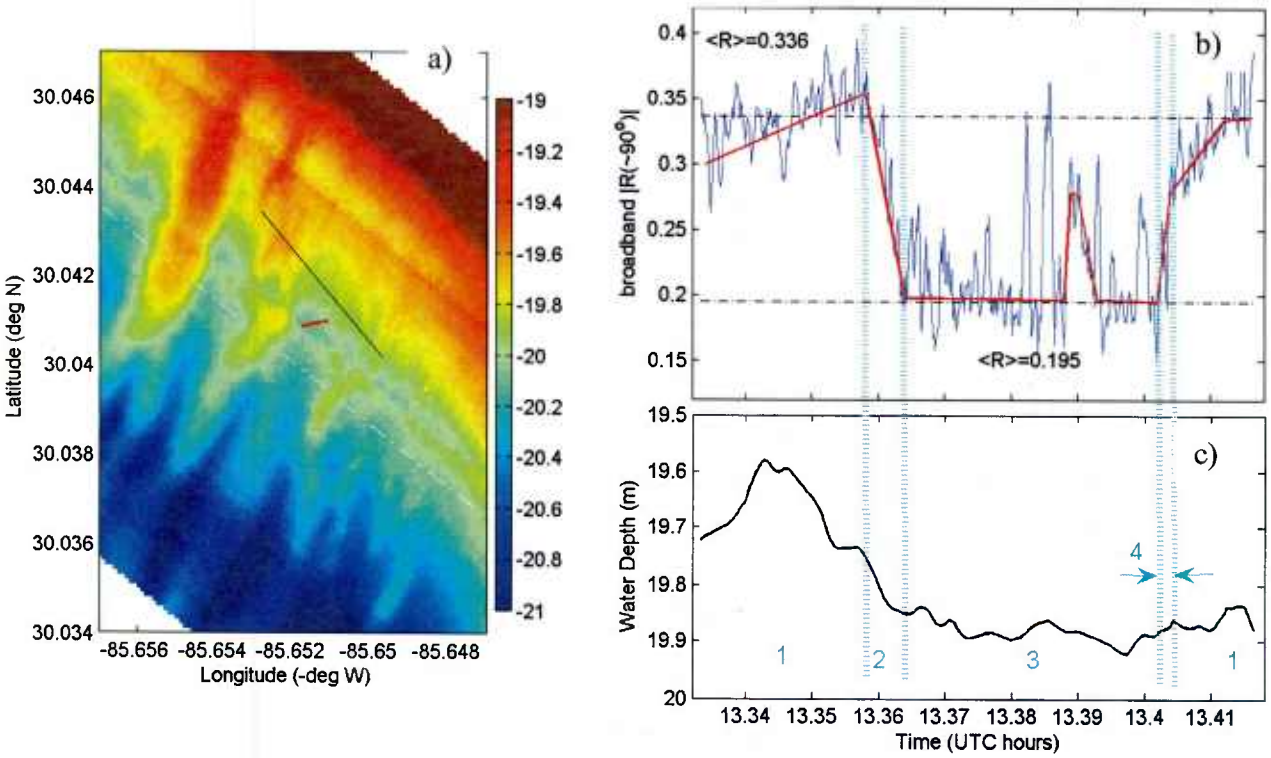

Figure 4. Bathymetry (left) in meters with normal incidence reflection track (black) trending southeast. The Site 2 wide-angle reflection track is shown in red trending west-southwest and the main reverberation line in white dash-dotted line. b) Normal incidence reflection coefficient data (blue) along with interpreted 'reflection regimes' (cyan dotted lines and numbers) and a smoothed fit (red) to the data. c) Along-track bathymetry (10 m resolution data from Chris DeMoustier and Barb Kraft). The tick mark spacing in time corresponds to ~55 meters in distance. The total track length is 440 m.

In an effort to understand the possible underlying geoacoustic variability along this track, the density and sound speed were first estimated at the average value of the simplest regimes 1 and 3 (shown in black dash-dotted line). It is well-known that there are numerous difficulties (i.e., ambiguities) in estimating density and sound speed from normal incidence reflection data. Reflection amplitudes are influenced by many mechanisms including roughness, sediment volume scattering, seafloor curvature, layering and impedance. Resolving individual contributions is generally not possible and for simplicity here all mechanisms are ignored except the latter, i.e., the seafloor is assumed to be a perfectly flat homogeneous halfspace for each consecutive ping. With this tacit assumption, it is possible to estimate the along-track sediment impedance Z (product of density and sound speed) knowing the seawater impedance Z_o

$$Z = Z_o\left(1+R(\pi/2)\right)\left(1-R(\pi/2)\right)^{-1}$$

From the impedance, the sediment sound speed and density are estimated from the empirical relations of Bachman [4]. These assumptions applied to Regime 1 (**R**=0.336) result in a sound speed of 1684

m/s and density of 1.87 g/cm^3 which compare well with the estimated sound speed (from the critical angle) of 1680 m/s from the wide-angle data at a ridge crest along the clutter track. The two crests are about 6 km apart, but the congruence of the sound speed suggests ridge crest geoacoustic properties may be similar in this region. In the swale, Regime 2 (**R**=0.195) yields a sound speed of 1544 m/s and a density of 1.68 g/cm^3. This is in concordance with the neaby Site 2 wide-angle measurements which indicated that the sound speed must be less than about 1585 m/s.

The fact that the approximate and average results in regime 1 and 2, do not appear to be in gross error, suggested that including all the regimes would not be unreasonable. In the present analysis, smoothing was performed such that only relatively large-scale fluctuations with a high probability of being related to geoacoustic variability were preserved. The smoothed reflection data for this part of the analysis is shown in Fig 4b in the red line.

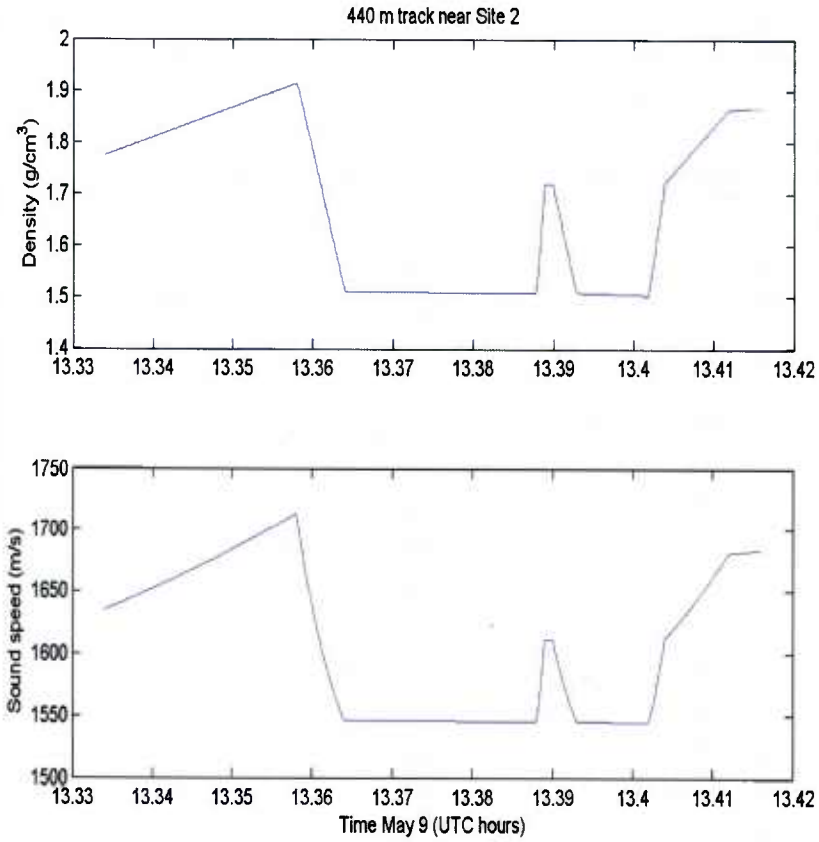

Figure 5. Estimated density and sound speed from smoothed normal incidence reflection data along a track (see red line in Figure 4b) from northwest to southeast near the TREX13 main reverberation line. The tick mark spacing in time is about 55 meters in distance.

The result of applying the flat homogeneous assumptions and the empirical equations to the spatially smoothed reflection data is shown in Fig 5. Note that there is a substantial variation in both density and sound speed across the short track. This is somewhat surprising given that the swale and crest differ in water depth only by 0.3 m. It is not understood at this time why the geoacoustic properties (impedance) increase from the ridge stoss side to the crest and then continue increasing until halfway down the lee side.

The lower sound speed and density in the swale (Regime 3) implies a higher concentration of clay and silt particles than on the ridge. In the swale there is a significant (ostensible) change in impedance at hour 13.39 which may represent a band of coarser grained sediment. The width of the band is about 22 m, which is comparable to the secondary peak in the spatial periodicity (at 43 m for a full cycle, 21.5 m for a half cycle or band). The lateral heterogeneity observed at 13.39 hr. is quite close to the wide angle reflection Site 2 location, and may be related to the (unknown) feature that yielded strong lateral heterogeneity at that site (see Fig 2a).

In summary the major observations from the wide angle $\mathbf{R}(\theta, f)$ and normal incidence $\mathbf{R}(\pi/2, f)$ reflection measurements are that

- There is a very distinct difference from sediments between ridge swale (main line) and ridge crest (clutter line) ($|R(\theta,f)|$)
- The geoacoustic properties at ridge crests are similar along the clutter line and main line (based on 1 correlation ($|R(\theta,f)|$ & $|R(\pi/2,f)|$)
- There are 4 distinct geoacoustic regimes that appear loosely correlated with bathymetry: stoss to lee side of crest, halfway down the lee side to the base of the swale, the swale, and the transition between the swale and the stoss side of the ridge crest. This was based on $|R(\pi/2,f)|$ only along one track.
- Strong geoacoustic variations occur in the swale ($|R(\pi/2,f)|$)
- Bulk density and sound speeds can be estimated with certain assumptions that do not seem unreasonable, ($|R(\pi/2,f)|$)
- There are strong lateral heterogeneities of order 1-10 m in sub-bottom, this was observed at both locations, Site C and Site 2 ($|R(\theta,f)|$)
- There are strong sediment lateral heterogeneities of order 10-100 m ($|R(\pi/2,f)|$)
- The lateral scales of sediment variability in this inner shelf environment (~20 m) is markedly different than lateral scales in (dozens of) measurements on mid to outer shelf environments, based on observations of layer resonance stationarity.

The observations raise a number of science questions:

- How does the TREX13 lateral heterogeneity at 1-10 m scale affect propagation? reverberation? (Since we can detect it, but not quantify it here we are unable to answer that question)
- What geologic processes are responsible for the detected lateral heterogeneity?
- Is the lateral heterogeneity we see here a "tip of the iceberg" in terms of a possible dominant scattering mechanism?
- Can information about the lateral heterogeneities be extracted from wide angle reflection data (an inverse point-of-view)? Inspection of the wide-angle data suggest that separating the intermingled angle and offset dependence may be possible in an objective probabilistic fashion exploiting sections of the data that are stationary, i.e., exhibit a resonance structure consistent with plane-layering. This would be a significant step to perform detailed geoacoustic estimation in areas of strongly lateral variability (this was not explored here).

IMPACT/APPLICATIONS

The derived geoacoustic model from the reflection data will aid in propagation, reverberation and clutter modeling. The strong sediment lateral variability has a number of implications. For example,

the 1-10 m scale lateral scales of sediment variability in this inner shelf environment are markedly different than lateral scales in dozens of reflections measurements conducted in mid to outer shelf environments. Thus, caution should be exercised in applying generalizations from TREX13 inner shelf observations to mid-to-outer shelf operational environments.

RELATED PROJECTS

ONR Seabed Geoacoustic Structure at the Meso-Scale: that project developed the machinery (forward models and inverse methods in collaboration with Jan Dettmer and Stan Dosso at UVic) for estimating geoacoustic properties and their frequency dependencies in complex, dispersive, layered media.

REFERENCES

[1] Holland C.W., Seabed reflection measurement uncertainty, J. Acoust. Soc. Am., 114, 1861-1873, 2003.

[2] Dettmer J., C.W. Holland and S.E. Dosso, Trans-dimensional uncertainty estimation for dispersive seabed sediments, Geophysics, 78, WB63-WB76, 2013.

[3] the analysis was performed on normalized data using a split window normalizer (averaging window of 9.5 m and a guard band of 12.75 m).

[4] Bachman R.T., Acoustic and physical property relationships in marine sediment, J. Acoust. Soc. Am., 78, 616, 1985.